JACC Vol. 13, No. 4
March 15, 1989:832–40

Feasibility of Identifying Amyloid and Hypertrophic Cardiomyopathy With the Use of Computerized Quantitative Texture Analysis of Clinical Echocardiographic Data

KRISHNASWAMY CHANDRASEKARAN, MD,* PHILIP E. AYLWARD, BM, PHD,†
STEVEN R. FLEAGLE, BSEE,†‡ TRUDY L. BURNS, PHD,§ JAMES B. SEWARD, MD, FACC,*‖
A. JAMIL TAJIK, MD, FACC,*‖ STEVE M. COLLINS, PHD,‡¶ DAVID J. SKORTON, MD, FACC,†‡
Rochester, Minnesota and Iowa City, Iowa

Ultrasound tissue characterization, the evaluation of certain physical properties of a tissue based on its acoustic properties, is an evolving application in echocardiography. The ability to identify acutely and chronically injured tissue has been demonstrated in a number of animal studies, but data in humans are limited. The present study tested the hypothesis that quantitative echocardiographic texture analysis, a method of evaluating the spatial pattern of echoes in echocardiographic images, would differentiate amyloid and hypertrophic cardiomyopathy from normal myocardium. Routine clinical echocardiographic data were obtained on 34 subjects at the Mayo Clinic (10 normal subjects, 10 patients with amyloid heart disease, 8 patients with hypertrophic cardiomyopathy and 6 patients with left ventricular hypertrophy due to hypertension). Standard videotape recordings of these echocardiograms were analyzed at the University of Iowa.

Echocardiographic data were digitized with use of a calibrated, 256 gray level digitization system. Quantitative texture analysis was performed on data from the ventricular septum and posterior left ventricular wall in end-diastolic and end-systolic, short-axis and long-axis echocardiographic images. The gray level run length texture variables were able to discriminate hypertrophic cardiomyopathy and amyloid heart disease from normal myocardium and from each other ($p < 0.0083$ for comparisons of the quantitative texture features of amyloid versus hypertrophic cardiomyopathy versus normal by multivariate analysis of variance). The texture of the myocardium in hypertensive left ventricular hypertrophy not associated with amyloid or hypertrophic cardiomyopathy was in general not significantly different from that of normal myocardium.

On the basis of these data, it was concluded that quantitative texture analysis of clinical echocardiographic data has the potential to identify amyloid and hypertrophic cardiomyopathy; false positive results occur rarely in left ventricular hypertrophy due to hypertension. Further prospective studies of this technique are needed to establish its utility in identifying the etiology of clinical cardiomyopathies.

(J Am Coll Cardiol 1989;13:832–40)

Ultrasound tissue characterization, the assessment of certain physical properties of biological tissue based on tissue acoustic properties, is a unique use of ultrasound with great potential for clinical diagnosis (1). This method of ultrasound analysis differs greatly from the standard clinical uses of echocardiography, which are directed at depicting the smooth surfaces of the heart (for example, endocardium or epicardium) to evaluate cardiac size, shape and function. Ultrasound myocardial tissue characterization research in vitro or using animal models has shown the ability of these

From the *Division of Cardiovascular Diseases and Internal Medicine and ‖Division of Pediatric Cardiology, Mayo Clinic, Rochester, Minnesota and the Cardiovascular Image Processing and Ultrasonic Imaging Laboratories, Cardiovascular Center and the †Departments of Internal Medicine, ‡Electrical and Computer Engineering, §Preventive Medicine and ¶Radiology, University of Iowa, Iowa City, Iowa. This study was supported in part by Grant HL07111-C, Program Project Grant 14388 and Specialized Center of Research (SCOR) in Ischemic Heart Disease Grant P50-HL32295 from the National Heart, Lung, and Blood Institute, National Institutes of Health, Bethesda, Maryland; American Heart Association-Iowa Affiliate Grant IAG-30, American Heart Association, West Des Moines, Iowa and the F. E. Rippel Foundation, Madison, New Jersey. Dr. Aylward was an Australian Heart Foundation Overseas Research Fellow, Woden, Australian Capital Territory 2606, Australia. Dr. Skorton is the recipient of Research Career Development Award K04-HL01290 from the National Heart, Lung, and Blood Institute, Bethesda, Maryland.

Manuscript received July 16, 1988; revised manuscript received October 26, 1988, accepted November 11, 1988.

Address for reprints: Philip E. Aylward, BM, Department of Cardiovascular Medicine, Flinders Medical Centre, Bedford Park, South Australia 5042, Australia.

0735-1097/89/$3.50

techniques to identify acutely ischemic (2–4), reperfused (3,5,6), infarcted (7–9), contused (10), fibrotic (11) and myopathic (12) myocardium. Sporadic observations in humans (13–15) have also been made, largely in the form of qualitative findings in clinical echocardiograms. For example, Rasmussen et al. (13) noted increased brightness of echo reflections from scarred tissue in patients with myocardial infarction. Martin et al. (14) commented on the unusual appearance of the septal myocardium in patients with hypertrophic cardiomyopathy. Similarly, Siqueira-Filho et al. (15) noted in the majority of patients with amyloid heart disease a peculiar "sparkling" texture to the myocardium. These qualitative observations have served as strong motivation for research in ultrasound tissue characterization because they supplied evidence that clinical abnormalities in myocardial microstructure could be associated with identifiable changes in echocardiographic acoustic properties. Although initial observations were recently made of ultrasound backscatter in dilated cardiomyopathy (16), relatively few data are available concerning quantitative aspects of tissue acoustic properties in human cardiac disorders in vivo.

We have recently developed an approach to ultrasound myocardial tissue characterization potentially applicable to clinical echocardiographic data. The approach consists of the quantitative analysis of the two-dimensional spatial pattern or "texture" of echocardiographic image data; we refer to the technique as quantitative texture analysis (10). Texture analysis has proved efficacious in identifying acutely ischemic (17,18) and contused (10) myocardium in animal models. Our purpose in the present study was to determine the potential of quantitative texture analytic techniques to discriminate normal from abnormal myocardium in clinical (human) cardiomyopathies. We chose as the subjects of our study patients with amyloidosis and hypertrophic cardiomyopathy—conditions in which myocardial microstructure is grossly disordered. Our hypothesis was that quantitative texture analysis would discriminate amyloid and hypertrophic cardiomyopathy from normal myocardium.

Methods

Study patients. The study group consisted of 10 normal subjects and 24 patients: 10 patients with amyloidosis, 8 with hypertrophic cardiomyopathy and 6 with left ventricular hypertrophy due to hypertension. These patients were referred to the echocardiographic laboratory at the Mayo Clinic for echocardiographic examination as part of their routine clinical evaluation. The diagnoses were made independently of the texture data on the basis of the following criteria.

Amyloidosis. All patients belonging to this group were diagnosed to have systemic amyloidosis by clinical features (19) confirmed by mucosal biopsy. Cardiac involvement was suspected when the following echocardiographic findings were present: 1) thickened right and left ventricular walls and ventricular septum, 2) normal or small left ventricular cavity size with normal or reduced systolic function, and 3) small pericardial effusion.

Hypertrophic cardiomyopathy. This entity was diagnosed on the basis of the following echocardiographic criteria: 1) asymmetric septal hypertrophy, 2) small hyperdynamic left ventricle, and 3) systolic anterior motion of the mitral valve apparatus.

Hypertensive left ventricular hypertrophy. This diagnosis was based on the presence of 1) concentrically thickened left ventricle (thickness >13 mm in all patients), 2) presence of long-standing systemic hypertension, and 3) absence of an infiltrative clinical disorder that could cause generalized thickening of the left ventricular walls.

Echocardiographic data acquisition. Two-dimensional echocardiograms were obtained with the use of standard techniques from conventional parasternal and apical acoustic windows (20). The instrument parameters (power output, time-gain compensation, gray scale transfer curves, and so forth) were adjusted to provide visually pleasing echocardiographic images. The data were analyzed retrospectively; that is, we evaluated routine, clinical echocardiograms performed in the usual fashion with no alterations in the standard methods of echo data acquisition. The images were obtained with the use of a mechanical sector scanner operating at 3 MHz (ATL Mark 600) in all patients as well as in normal subjects. The images were recorded on 0.75 in. (2 cm) videocassette tape with the use of a U-matic videocassette recorder (Sony).

Standard echocardiographic analysis. With use of the conventions suggested by the American Society of Echocardiography (21), the following measurements were obtained: end-diastolic thickness of the posterior left ventricular wall and ventricular septum, end-diastolic and end-systolic minor axis dimensions of the left ventricular cavity and fractional shortening and ejection fraction of the left ventricle.

Echocardiographic data digitization. Echocardiographic images recorded on videotape were digitized with the use of a calibrated video digitization system. The video output of the videocassette recorder was connected to a digital time-base corrector (Harris Corp., model 516WB), a device that corrects for time-base instabilities in the video signal that result from the usual variations in videocassette tape speed. The analog output of the time-base corrector before video digitization was adjusted so that the video signal for each echocardiographic study occupied the entire dynamic range of the digitizer. The time-base–corrected analog video signal was digitized into a 512 × 512, 8-bit (256 gray level) digital array with use of a commercial real-time video digitizer (Gould IP-8500). While viewing the real-time two-dimensional echocardiographic digital display, the observer triggered the capture (digital storage) of 16 video frames. These frames were then viewed by two observers and, by consensus, end-diastolic and end-systolic frames were chosen. End-

diastole was defined as the frame closest to the peak of the electrocardiographic (ECG) R wave; end-systole was chosen as the frame with the smallest apparent left ventricular cavity area. The digitization procedure was performed on parasternal long- and short-axis views. Thus, at the end of the digitization procedure, digital echocardiographic data were stored representing long- and short-axis echocardiographic views of each subject at end-diastole and end-systole.

Quantitative texture analysis. Regions of interest for texture analysis were chosen by consensus of two (nonblinded) observers using an interactive computer program. With use of a trackball-controlled cursor, rectangular regions of interest were placed in the ventricular septum and posterior left ventricular wall in short- and long-axis images acquired at end-diastole and end-systole. The rectangular regions of interest were made as large as possible while excluding reflections from the endocardium and epicardium. The data from each region of interest were analyzed with use of measures related to the intensity and distribution of echo amplitude (gray levels) within the region of interest. The variables that we used in the present study can be categorized into two families: 1) gray level run length measures and 2) gray level difference measures.

Gray level run length measures. A gray level run is defined as a set of consecutive, collinear pixels having the same gray level value or gray level values within a given range (22). The length of a run is characterized by the number of pixels traversed before a significant change in gray level value is encountered. For each image region, we calculated a gray level run length matrix p(i, j) in which each matrix element specified the number of runs of gray level i and length j. We computed the run-length matrix for runs in both the horizontal (0°) and vertical directions (90°). A run was assigned to gray level i if all pixels in the run had a gray level in the interval [(i − 1)*32, i*32 − 1]. A run was assigned a length j if the number of pixels in the run was in the jth interval in the following list: {1, 2–3, 4–6, 7–10, 11–15, 16–80}. *Five gray level run length variables were calculated from the matrix p(i, j):*

1) *Long run emphasis:*

$$\text{LRE} = \sum_{i=1}^{8}\sum_{j=1}^{6} j^2 p(i,j) \Big/ \sum_{i=1}^{8}\sum_{j=1}^{6} p(i,j). \quad [1]$$

2) *Short run emphasis:*

$$\text{SRE} = \sum_{i=1}^{8}\sum_{j=1}^{6} \frac{p(i,j)}{j^2} \Big/ \sum_{i=1}^{8}\sum_{j=1}^{6} p(i,j). \quad [2]$$

3) *Gray level nonuniformity:*

$$\text{GLN} = \sum_{i=1}^{8}\left(\sum_{j=1}^{6} p(i,j)\right)^2 \Big/ \sum_{i=1}^{8}\sum_{j=1}^{6} p(i,j). \quad [3]$$

4) *Run length nonuniformity:*

$$\text{RLN} = \sum_{j=1}^{6}\left(\sum_{i=1}^{8} p(i,j)\right)^2 \Big/ \sum_{i=1}^{8}\sum_{j=1}^{6} p(i,j). \quad [4]$$

5) *Run percentage:*

$$\text{RP} = \sum_{i=1}^{8}\sum_{j=1}^{6} p(i,j)/P. \quad [5]$$

In the last equation, P is the number of pixels in the region of interest (maximal possible number of runs). Gray level run length variables can be conceptualized as measures of the heterogeneity of gray levels and of the relative size of individual echo reflections within each echocardiographic region of interest (23).

Gray level difference measures. The gray level difference variables are also measures of the heterogeneity of the distribution of echocardiographic reflections within each tissue region of interest (24). These variables are derived by measuring the absolute difference in image gray level value between image picture points separated by various numbers of pixels in horizontal and vertical directions. In the present study, we calculated a 256-dimensional histogram, $p_\Delta(i)$, whose ith component was the probability that two pixels with a separation of Δ had an absolute difference in gray level of i. We calculated this histogram for separations of 1, 2, 4 and 8 pixels in each direction. *The following variables were derived from $p_\Delta(i)$:*

1) Contrast (CON):

$$\text{CON} = \sum_{i=1}^{256} i^2 p_\Delta(i). \quad [6]$$

2) Angular second moment (ASM):

$$\text{ASM} = \sum_{i=1}^{256} p_\Delta(i)^2. \quad [7]$$

3) Entropy (ENT):

$$\text{ENT} = -\sum_{i=1}^{256} p_\Delta(i) * \log\left(p_\Delta(i)\right). \quad [8]$$

4) Mean:

$$\text{Mean} = (1/256)\sum_{i=1}^{256} i * p_\Delta(i). \quad [9]$$

The four gray level difference variables characterize the shape of the gray level difference histogram (24).

Table 1. Results of Standard Echocardiographic Analyses in 34 Cases*

Group	n	M	F	Age (yr)	PW (mm)	VS (mm)	LVD_d (mm)	LVD_s (mm)	Fr. Short (%)	EF (%)
Amyloid	10	6	4	66 ± 11	17.2 ± 3.1	18.3 ± 2.6	45.3 ± 8.4	33.2 ± 8.2	27.3 ± 9.0	46.8 ± 1
				(50 to 88)	(14 to 22)	(15 to 22)	(34 to 62)	(20 to 47)	(13 to 43)	(25 to 68)
HCM	8	4	4	40 ± 21	11.6 ± 2.6	24.8 ± 5.6	38.8 ± 4.0	19.3 ± 3.2	50.3 ± 4.8	75.6 ± 4
				(17 to 70)	(7 to 15)	(17 to 33)	(31 to 42)	(14 to 23)	(45 to 56)	(70 to 81)
LVH	6	4	2	46 ± 23	12.8 ± 1.5	12.8 ± 1.9	50.5 ± 7.6	32.3 ± 8.0	36.0 ± 11	59.3 ± 1
				(17 to 74)	(11 to 15)	(10 to 15)	(39 to 60)	(28 to 48)	(17 to 44)	(35 to 69)
Normal	10	4	6	29 ± 10	8.3 ± 1.4	8.3 ± 1.4	46.6 ± 6	27.7 ± 3.6	39.6 ± 5.1	64.7 ± 6
				(16 to 44)	(6 to 10)	(6 to 10)	(31 to 54)	(19 to 33)	(33 to 46)	(55 to 72)

*Values are mean ± SD. Range is in parentheses. EF = ejection fraction; F = female; Fr. Short = percent change in minor axis dimension; HCM = hypertrophic cardiomyopathy; LVD_d = left ventricular end-diastolic minor axis dimension; LVD_s = left ventricular end-systolic minor axis dimension; LVH = hypertensive left ventricular hypertrophy; M = male; n = total number of patients; PW = posterior left ventricular wall thickness; VS = ventricular septal thickness.

Statistical analysis. Our null hypothesis was that there were no texture differences among the four study groups. This hypothesis was tested with the use of multivariate analysis of variance, followed by pairwise group comparisons among the amyloid, hypertrophic cardiomyopathy, hypertensive left ventricular hypertrophy and normal groups. The six comparisons among the groups were made within each region of interest by time in the cardiac cycle and by echocardiographic view. A p value ≤ 0.0083 (0.05/6) was considered significant with the use of the Bonferroni method of correction (25).

Results

Clinical echocardiographic information. The results of standard echocardiographic measurements are given in Table 1. The three patient groups all demonstrated significant thickening of the left ventricular posterior wall and of the ventricular septum compared with values in the normal group ($p < 0.01$). There was no statistically significant difference in wall thickness among the three patient groups. Apart from the amyloid group, the ejection fraction was either normal or hyperdynamic. The echocardiographic image texture by visual observation was distinctive in the amyloid group; no difference was noticed among the visual textures of the myocardium in hypertrophic cardiomyopathy, hypertensive left ventricular hypertrophy and normal subjects (Fig. 1).

Quantitative Texture Analysis

The results of quantitative texture analysis using gray level run length and gray level difference measures are shown in Figures 2 to 4.

Gray level run length measures. These texture measures were able to differentiate the echo data of the ventricular septum of hypertrophic cardiomyopathy from that of amyloid cardiomyopathy, left ventricular hypertrophy secondary to hypertension and normal myocardium (Fig. 2A and 3A). Similarly the septal texture of amyloid myocardium was different from that of normal myocardium (Fig. 2A and 3A). These differences were consistent when data were evaluated from different image orientations, at both points in the cardiac cycle, and when calculated in horizontal and vertical directions. In particular, gray level nonuniformity differentiated among hypertrophic cardiomyopathy, amyloid, normal and hypertrophy in both views, in both calculation directions and at both points in the heart cycle.

Texture measures derived from the posterior wall echo data were able to differentiate amyloid disease (which involves the myocardium diffusely) from normal myocardium and hypertensive hypertrophy but did not show differences between the uninvolved posterior wall of hypertrophic cardiomyopathy compared with that of left ventricular hypertrophy (Fig. 2B and 3B). In general, the texture measures calculated perpendicular to the ultrasound beam direction (0°) were more sensitive in identifying the differences noted. In none of the comparisons utilizing gray level run length measures was the texture of hypertensive left ventricular hypertrophy significantly different from normal.

Gray level difference measures. The gray level difference texture measures that differentiated among our study groups are shown in Figure 4. It can be noted that these measures were much less effective at discriminating among the cardiomyopathies than the gray level run length measures. In 11 of 256 comparisons (4%) utilizing gray level difference measures, the texture of hypertensive left ventricular hypertrophy was significantly different than normal.

Discussion

The major finding of our study was that quantitative texture analysis permitted discrimination of the abnormal myocardium of amyloidosis and hypertrophic cardiomyopa-

JACC Vol. 13, No. 4
March 15, 1989:832–40

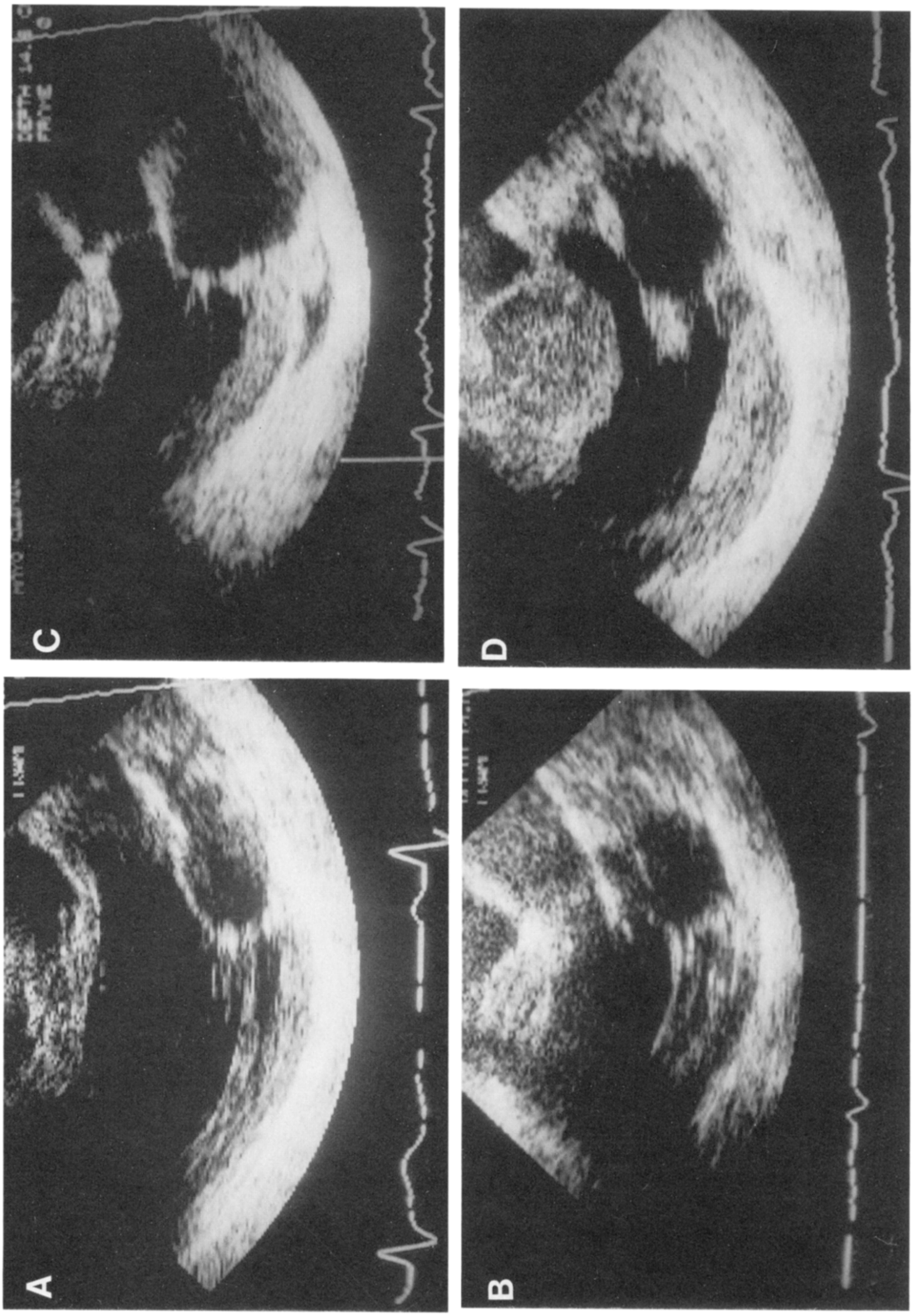

Figure 1. Representative echocardiographic images of the patient groups evaluated. The images are parasternal long-axis views of a normal heart (**A**) and of hearts with hypertensive left ventricular hypertrophy (**B**), amyloidosis (**C**) and hypertrophic cardiomyopathy (**D**).

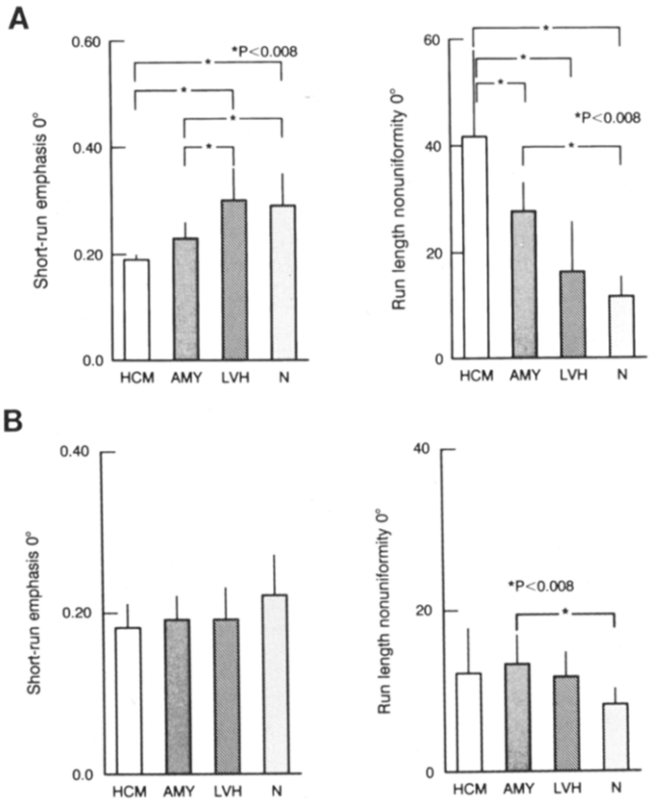

Figure 2. Selected gray level run length data from end-diastolic long-axis views of the ventricular septum (**A**) and the posterior left ventricular wall (**B**). In each panel, the graphs show mean data (± SD) for short run emphasis (**left**) and run length nonuniformity (**right**), both calculated along the 0° (horizontal) direction (that is, perpendicular to the ultrasound beam). These run length variables demonstrated significant differences among hypertrophic cardiomyopathy (HCM), amyloidosis (AMY) and normal myocardium (N) in the ventricular septum (A) and between amyloidosis and normal myocardium in the posterior wall (B). LVH = hypertensive left ventricular hypertrophy.

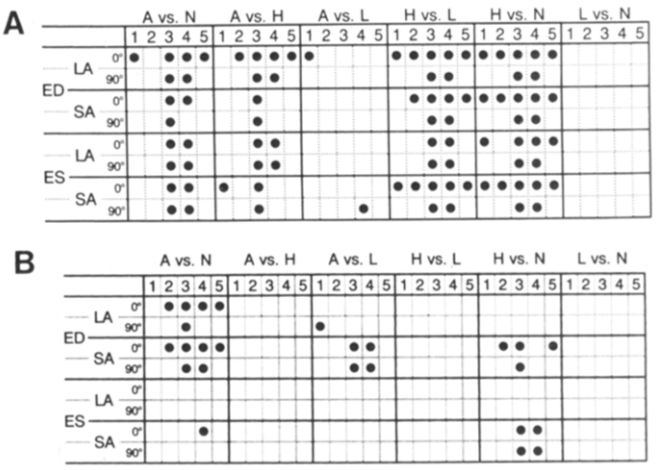

Figure 3. Gray level run length measures showing statistically significant differences in paired comparisons among the various patient groups for echocardiographic data obtained from the ventricular septum (**A**) and posterior left ventricular wall (**B**). The numbers 1 to 5 indicate the specific gray level run length texture measures: 1 = short run emphasis; 2 = long run emphasis; 3 = gray level nonuniformity; 4 = run length nonuniformity; 5 = run percentage. The presence of a **solid dot** in a particular cell in the graph indicates that a significant difference was found for that intergroup comparison for the particular texture measure indicated. A = amyloid; ED = end-diastole; ES = end-systole; H = hypertrophic cardiomyopathy; L = left ventricular hypertrophy; LA = long axis; N = normal; SA = short axis; 0° = texture calculated in the horizontal direction (perpendicular to beam); 90° = vertical (parallel to beam).

thy from normal tissue. Our analysis was performed on standard, clinical echocardiographic images that were recorded on videotape, suggesting the potential clinical applicability of the method. In this discussion, we will review some of the basis for echocardiographic texture analysis, its applicability in cardiomyopathy, some of the limitations of our approach, and some clinical implications of our findings.

Echocardiographic texture analysis. Texture is an important diagnostic feature in an ultrasound image (26). Qualitative observations of standard echocardiograms commonly reveal abnormalities of image texture in conditions associated with alterations in myocardial composition or myofibrillar architecture, or both (13–15). In a B-mode ultrasound image, the spatial distribution of the returning echo signal gives rise to the apparent texture, which results from acoustic speckle (27,28). The acoustic speckle in echocardiograms results from constructive and destructive interference of ultrasound reflected from many myocardial microstructures. Therefore, the spatial pattern of speckle bears a complex and indirect relation to the specific internal architecture of the myocardium. Some investigators have shown some correspondence between the speckle pattern and certain structural characteristics of the myocardium. Bhandari and Nanda (29) showed that the pattern of myocardial echoes seen on echocardiographic images bore a definite relation to histologic abnormalities. Further, the abnormal texture of ischemic myocardium on compound B-scan images demonstrates the potential diagnostic value of texture analysis (4).

The ability of the human observer to precisely characterize changes in visual texture is limited. Hence, various investigators (22,24) have used digital computer analysis methods to estimate the quantitative characteristics of image texture. These texture measures are in general based on statistical descriptors of the spatial distribution of gray levels; these measures appear to be better discriminators of texture than are simple histogram statistics (30,31). Texture measures have been found capable of discriminating normal from contused (10) and ischemic myocardium (17,18) in animal experiments and were able to differentiate among intracardiac masses (32) in humans. Lloret et al. (33) differentiated embolic from nonembolic thrombi by quantitative texture analysis.

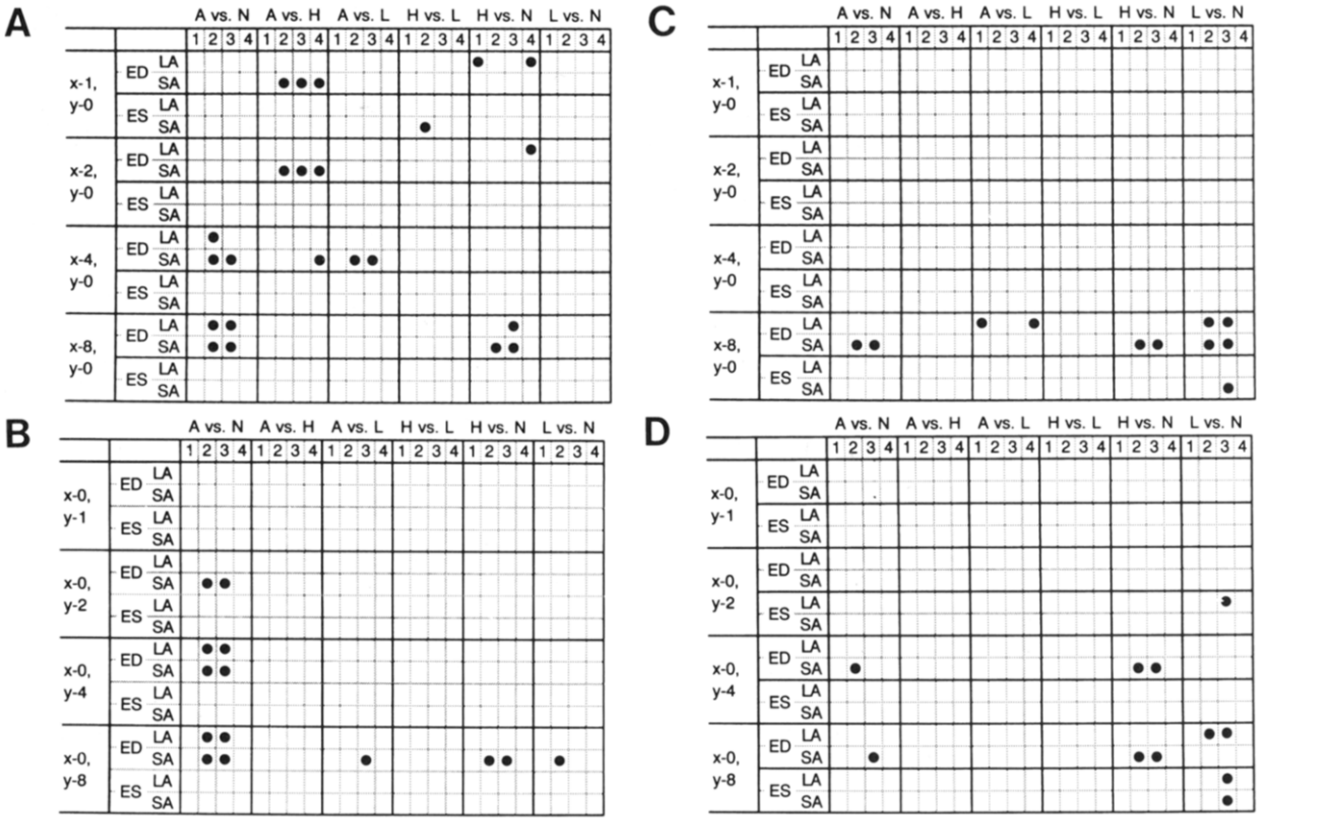

Figure 4. Gray level difference measures exhibiting significant differences in paired comparisons among the various patient groups. The graphs show significant intergroup differences for gray level difference texture measures calculated in the horizontal (0°) direction for the ventricular septum (**A**), in the vertical (90°) direction for the septum (**B**), in the horizontal direction for the posterior left ventricular wall (**C**) and in the vertical direction for the posterior wall (**D**). The numbers 1 to 4 indicate specific gray level difference texture measures: 1 = contrast; 2 = angular second moment; 3 = entropy; 4 = mean. x and y indicate interpixel spacings in the horizontal and vertical directions, respectively, at which gray level differences were measured. Other abbreviations as in Figure 3.

Texture analysis in cardiomyopathy. Hypertrophic cardiomyopathy is a genetically inherited disorder characterized by altered myocardial microstructure, including hypertrophy and disorganization of myofibrils along with fibrosis (34). In its usual presentation, it is easily diagnosed by standard echocardiography. In addition to gross morphologic abnormalities, Martin et al. (14) observed a "ground-glass" texture on echo images in the septal region of patients with this disorder and attributed it to altered myocardial structure. However, their finding of altered echo texture was not described in some other studies (35). In the present study, we did not routinely notice unusual echo texture in the septal region of patients with hypertrophic cardiomyopathy. Nevertheless, the *quantitative* texture features of the septal echo data in long- and short-axis, systolic and diastolic images, differentiated hypertrophic myopathy from the other groups in our study. We believe that the alteration in texture is related in part to altered myofibrillar architecture or fibrosis, or both, in the septum of these hearts as previously demonstrated by histologic studies (36–39). Tanaka et al. (37) estimated the extent of fibrosis in hypertrophic cardiomyopathy, in hypertensive hearts and in normal hearts. The percent area of fibrosis in the left ventricular wall was significantly increased in hypertrophic cardiomyopathy (10.5 ± 4.3%) compared with that in hypertensive hypertrophy (2.6 ± 1.5%) and normal heart (1.1 ± 0.5%).

Amyloid infiltration of myocardium results in a restrictive cardiomyopathy. Histologically, amyloid infiltration causes myocardial fiber necrosis, atrophy and fibrosis, leaving empty amyloid rings or solid sheets of amyloid (40). Amyloid deposits within the myocardium may cause an acoustic impedance mismatch, resulting in increased echo intensity. These increased echo intensities seen diffusely throughout the myocardium have been described by some investigators (15) as "granular sparkling" in appearance. In the present study, the texture data from the septum and posterior wall differentiated amyloid from normal myocardium and hypertrophic myopathy but not from hypertensive hypertrophy.

The inability of the texture measures we employed to differentiate the echo data from the relatively uninvolved posterior wall of hypertrophic cardiomyopathy from the posterior wall data of hypertensive left ventricular hypertrophy and from normal myocardium (there is no gross change

in the microstructure of the posterior wall of hypertrophic cardiomyopathy) emphasizes the reliability of these measures and, hence, the results.

Limitations and clinical implications. At present, the texture measures we employed were able to discriminate hypertrophic cardiomyopathy from normal myocardium, hypertensive hypertrophy and amyloid disease; amyloid-infiltrated myocardium was distinguished to a lesser extent from hypertensive hypertrophy and normal myocardium. However, these quantitative texture measures did not in general differentiate hypertensive hypertrophy from normal myocardium. The ability of texture analysis to discriminate hypertrophic cardiomyopathy may play a significant role in clinical situations where hypertrophic myopathy may simulate infiltrative myocardial disease (41), hypertensive heart disease in elderly patients may mimic hypertrophic cardiomyopathy (42) and cardiac amyloidosis may resemble hypertrophic myopathy (43–45).

Although our preliminary results in human cardiomyopathy seem promising, there are important problems that remain to be solved before quantitative texture analysis can be widely used clinically. Texture (speckle) characteristics are markedly influenced by the characteristics of the ultrasound imaging system (46,47); we tried to minimize this effect by analyzing echo images obtained from a single ultrasound scanning system. The limited amplitude dynamic range and nonlinear data compression in commercial ultrasound instruments cause alterations of regional echo amplitude information, which may mimic or mask "diagnostic" changes in ultrasound texture. Problems are also incurred by the standard methods of depth-gain compensation. For optimal ultrasound tissue characterization, the gain compensation profile should exactly match the attenuation profile produced by the several tissues encountered by the interrogating beam. Current methods of gain compensation do not allow for the necessary individual compensation profiles along each of the lines of sight used to make up a two-dimensional echocardiographic image. Even with several independent gain controls, the gain compensation chosen at any given depth is applied to all lines of the image at that depth, irrespective of the tissue path each line has encountered. This procedure may result in artificial regional differences in gray level data (48). These and other instrumentation-related sources of variability underscore the need for methods of standardizing instrument settings. Further investigations utilizing such standardized adjustments will be necessary before more widespread clinical use of texture analysis will be possible. The design of the present study did not permit us to systematically evaluate the effect of instrument adjustments on echo image texture nor to propose methods of standardizing these adjustments.

Although the gray level difference measures from septal echo data were able to differentiate amyloid from hypertrophic cardiomyopathy and from normal myocardium, this class of texture measures was relatively insensitive compared with the gray level run length calculations. We are uncertain as to the reason for this differential sensitivity. One possible explanation is based on our specific implementation of the texture calculations in this study. The efficacy of the gray level difference measures depends largely on the interpixel spacing at which gray level differences are measured. Because we had no previous knowledge of the specific changes in texture that might be expected, our choice of interpixel spacings (1, 2, 4 and 8 pixels) may not have produced an optimal match with actual texture alterations.

Conclusions. We have shown that quantitative texture analytic measures have the potential to distinguish normal from myopathic myocardium and to discriminate between infiltrative and hypertrophic processes on the basis of standard videotaped echocardiographic data. The known dependence of ultrasound image data on imaging system characteristics necessitates further testing of the robustness of this approach with use of other echocardiographic systems before further clinical use can be suggested. In addition, comparisons of texture analysis with other methods of tissue characterization (2,6,8) in cardiomyopathy would be of interest. Successful completion of further clinical studies may supply the clinician with an additional tool useful in the diagnosis of cardiomyopathies.

We acknowledge Barbara Manahan and Julie Haugen, BSEE for technical assistance and Kay Witte, Carolyn Frisbie, Rita Yeggy and Rita Griffin for expert preparation of the manuscript.

References

1. Miller JG, Pérez JE, Sobel BE. Ultrasonic characterization of myocardium. Prog Cardiovasc Dis 1985;28:85–110.
2. Mimbs JW, Bauwens D, Cohen RD, O'Donnell M, Miller JG, Sobel BE. Effects of myocardial ischemia on quantitative ultrasonic backscatter and identification of responsible determinants. Circ Res 1981;49:89–96.
3. Rasmussen S, Lovelace DE, Knoebel SB, Ransburg R, Corya BC. Echocardiographic detection of ischemic and infarcted myocardium. J Am Coll Cardiol 1984;3:733–43.
4. Chandrasekaran K, Greenleaf JF, Robinson BS, Edwards WD, Seward JB, Tajik AJ. Echocardiographic visualization of acute myocardial ischemia: in vitro study. Ultrasound Med Biol 1986;12:785–93.
5. Glueck RM, Mottley JG, Miller JG, Sobel BE, Pérez JE. Effects of coronary artery occlusion and reperfusion on cardiac cycle-dependent variation of myocardial ultrasonic backscatter. Circ Res 1985;56:683–9.
6. Haendchen RV, Ong K, Fishbein MC, Zwehl W, Meerbaum S, Corday E. Early differentiation of infarcted and noninfarcted reperfused myocardium in dogs by quantitative analysis of regional myocardial echo amplitudes. Circ Res 1985;57:718–28.
7. Gramiak R, Waag RC, Schenk EA, Lee PK, Thomson K, Macintosh P. Ultrasonic detection of myocardial infarction by amplitude analysis. Radiology 1979;130:713–20.
8. Skorton DJ, Melton HE Jr, Pandian NG, et al. Detection of acute myocardial infarction in closed-chest dogs by analysis of regional two-dimensional echocardiographic gray-level distributions. Circ Res 1983;52:36–44.

9. Mimbs JW, Yuhas DE, Miller JG, Weiss AN, Sobel BE. Detection of myocardial infarction in vitro based on altered attenuation of ultrasound. Circ Res 1977;41:192–8.

10. Skorton DJ, Collins SM, Nichols J, Pandian NG, Bean JA, Kerber RE. Quantitative texture analysis in two-dimensional echocardiography: application to the diagnosis of experimental myocardial contusion. Circulation 1983;68:217–23.

11. Hoyt RH, Collins SM, Skorton DJ, Ericksen EE, Conyers D. Assessment of fibrosis in infarcted human hearts by analysis of ultrasonic backscatter. Circulation 1985;71:740–4.

12. Pérez JE, Barzilai B, Madaras EI, et al. Applicability of ultrasonic tissue characterization for longitudinal assessment and differentiation of calcification and fibrosis in cardiomyopathy. J Am Coll Cardiol 1984;4:88–95.

13. Rasmussen S, Corya BC, Feigenbaum H, Knoebel SB. Detection of myocardial scar tissue by M-mode echocardiography. Circulation 1978;57:230–7.

14. Martin RP, Rakowski H, French J, Popp RL. Idiopathic hypertrophic subaortic stenosis viewed by wide angle, phased-array echocardiography. Circulation 1979;59:1206–17.

15. Siqueira-Filho AG, Cunha CLP, Tajik AJ, Seward JB, Schattenberg TT, Giuliani ER. M-mode and two-dimensional echocardiographic features in cardiac amyloidosis. Circulation 1981;63:188–96.

16. Vered Z, Barzilai B, Mohr GA, et al. Quantitative ultrasonic tissue characterization with real-time integrated backscatter imaging in normal human subjects and in patients with dilated cardiomyopathy. Circulation 1987;76:1067–73.

17. Chandrasekaran K, Chu A, Greenleaf JF, et al. 2D echo quantitative texture analysis of acutely ischemic myocardium (abstr). Circulation 1986;74(suppl II):II-271.

18. McPherson DD, Aylward PE, Knosp BM, et al. Ultrasound characterization of acute myocardial ischemia by quantitative texture analysis. Ultrason Imaging 1986;8:227–40.

19. Rubinow A. Amyloidosis. In: Stein JH, ed. Internal Medicine. 2nd ed. Boston: Little, Brown, 1987:1354–7.

20. Tajik AJ, Seward JB, Hagler DJ, Mair DD, Lie JT. Two-dimensional real-time ultrasonic imaging of the heart and great vessels: technique, image orientation, structure identification, and validation. Mayo Clin Proc 1978;53:271–303.

21. Sahn DJ, DeMaria A, Kisslo J, Weyman A. Recommendations regarding quantitation in M-mode echocardiography: results of a survey of echocardiographic measurements. Circulation 1978;58:1072–83.

22. Galloway MW. Texture analysis using gray level run lengths. Computer Graphics and Image Processing 1975;4:172–9.

23. Collins SM, Skorton DJ, Prasad NV, Olshansky B, Bean JA. Quantitative echocardiographic image texture: normal contraction-related variability. IEEE Trans Med Imag 1985;MI-4:185–92.

24. Weszka JS, Dyer CR, Rosenfeld A. A comparative study of texture measures for terrain classification. IEEE Trans Syst Man Cyber 1976;SMC-6:269–85.

25. Wallenstein S, Zucker CL, Fleiss JL. Some statistical methods useful in circulation research. Circ Res 1980;47:1–9.

26. Kossoff G, Garrett WJ, Carpenter DA, Jellins J, Dadd MJ. Principles and classification of soft tissues by grey scale echography. Ultrasound Med Biol 1976;2:89–105.

27. Wells PNT, Halliwell M. Speckle in ultrasonic imaging. Ultrasonics 1981;19:225–9.

28. Abbott JG, Thurstone FL. Acoustic speckle: theory and experimental analysis. Ultrason Imaging 1979;1:303–24.

29. Bhandari AK, Nanda NC. Two-dimensional echocardiographic recognition of abnormal changes in the myocardium. Ultrasound Med Biol 1982;8:663–71.

30. Mailloux GE, Bertrand M, Stampfler R, Ethier S. Texture analysis of ultrasound B-mode images by segmentation. Ultrason Imaging 1984;6:262–77.

31. Nicholas D, Nassiri DK, Garbutt P, Hill CR. Tissue characterization from ultrasound B-scan data. Ultrasound Med Biol 1986;12:135–43.

32. Chandrasekaran K, Chu A, Nimmagadda RR, Greenleaf JF, Seward JB, Tajik AJ. Texture analysis of intracardiac masses (abstr). Ultrason Imaging 1986;8:38.

33. Lloret RL, Cortada X, Bradford J, Metz MN, Kinney EL. Classification of left ventricular thrombi by their history of systemic embolization using pattern recognition of two-dimensional echocardiograms. Am Heart J 1985;110:761–5.

34. Epstein SE, Henry WL, Clark CE, et al. Asymmetric septal hypertrophy. Ann Intern Med 1974;81:650–8.

35. Maron BJ, Epstein SE. Hypertrophic cardiomyopathy: recent observations regarding the specificity of three hallmarks of the disease: asymmetric septal hypertrophy, septal disorganization and systolic anterior motion of the anterior mitral leaflet. Am J Cardiol 1980;45:141–54.

36. Nunoda S, Genda A, Sekiguchi M, Takeda R. Left ventricular endomyocardial biopsy findings in patients with essential hypertension and hypertrophic cardiomyopathy with special reference to the incidence of bizarre myocardial hypertrophy with disorganization and biopsy score. Heart Vessels 1985;1:170–5.

37. Tanaka M, Fujiwara H, Onodera T, Wu DJ, Hamashima Y, Kawai C. Quantitative analysis of myocardial fibrosis in normals, hypertensive hearts, and hypertrophic cardiomyopathy. Br Heart J 1986;55:575–81.

38. Isner JM, Maron BJ, Roberts WC. Comparison of amount of myocardial cell disorganization in operatively excised septectomy specimens with amount observed at necropsy in 18 patients with hypertrophic cardiomyopathy. Am J Cardiol 1980;46:42–7.

39. Unverferth DV, Baker PB, Pearce LI, Lautman J, Roberts WC. Regional myocyte hypertrophy and increased interstitial myocardial fibrosis in hypertrophic cardiomyopathy. Am J Cardiol 1987;59:932–6.

40. Batsakis JG. Degenerative lesions of the heart. In: Gould SE, ed. Pathology of the Heart and Blood Vessels. 3rd ed. Springfield, IL: Charles C Thomas, 1968:479–526.

41. Frustaci A, Loperfido F, Pennestri F. Hypertrophic cardiomyopathy simulating an infiltrative myocardial disease. Br Heart J 1985;54:329–32.

42. Topol EJ, Traill TA, Fortuin NJ. Hypertensive hypertrophic cardiomyopathy of the elderly. N Engl J Med 1985;312:277–83.

43. Griffiths BE, Hughes P, Dowdle R, Stephens MR. Cardiac amyloidosis with asymmetrical septal hypertrophy and deterioration after nifedipine. Thorax 1982;37:711–2.

44. Sedlis SP, Saffitz JE, Schwob VS, Jaffe AS. Cardiac amyloidosis simulating hypertrophic cardiomyopathy. Am J Cardiol 1984;53:969–70.

45. Oh JK, Tajik AJ, Edwards WD, Bresnahan JF, Kyle RA. Dynamic left ventricular outflow tract obstruction in cardiac amyloidosis detected by continuous-wave Doppler echocardiography. Am J Cardiol 1987;59:1008–10.

46. Flax SW, Glover GH, Pelc NJ. Textural variations in B-mode ultrasonography: a stochastic model. Ultrason Imaging 1981;3:235–57.

47. Kimme-Smith C, Jones JP. The relative effects of system parameters on texture in gray-scale ultrasonograms. Ultrasound Med Biol 1984;3:299–307.

48. Melton HE Jr, Skorton DJ. Rational gain compensation for attenuation in cardiac ultrasonography. Ultrason Imaging 1983;5:214–28.